Two and three-dimensional numerical modelling of flow patterns in shallow rectangular reservoirs

El Mehdi CHAGDALI[1,2], Cédric GOEURY[2], Jacques FONTAINE[2], Matthieu SECHER[3], Sébastien ERPICUM[4], Benjamin DEWALS[4], Kamal EL KADI ABDERREZZAK[1,2]

[1] EDF R&D, National Laboratory for Hydraulics and Environment, France

[2] Saint Venant Laboratory for Hydraulics, University Paris-Est, France

[3] EDF Hydro – CIH, France

[4] University of Liege (ULg), Research Group of Hydraulics in Environmental and Civil Engineering, Belgium

Email: el-mehdi.chagdali@edf.fr

Abstract*—Two- and three-dimensional numerical models TELEMAC-2D and TELEMAC-3D are used for simulating laboratory experiments of steady flow in shallow rectangular reservoirs. Using TELEMAC-2D, various user-defined parameters and options are tested. In particular, six turbulence models are evaluated, along with a grid size sensitivity. Using the finite element and finite volume approaches, several numerical schemes for solving the advection step for velocity and turbulence are compared. For all laboratory configurations, the measured and computed horizontal velocity fields are compared. Satisfactory results are obtained with TELEMAC-2D using the Spalart-Allmaras turbulence model. The effect of numerical scheme is very weak. A comparison between TELEMAC-2D and TELEMAC-3D is performed using the k–ε turbulence model with LIPS scheme for the particular C-C reservoir configuration. The 3D simulations slightly improve the results.

I. INTRODUCTION

The loss of effective storage capacity in shallow reservoirs due to sediment accumulation decreases reservoir's functionality for flood control, hydropower generation, irrigation and water supply. Sedimentation within these reservoirs depends on the flow, which can exhibit different patterns depending on the reservoir shape, boundary conditions and sediment input characteristics [4, 10]. The flow field can feature symmetric and asymmetric patterns with reattachment points [7] or a meandering jet [8]. Optimal design and management of shallow reservoirs need accurate prediction of the sedimentation areas and thickness, which can be supported by detailed analyses of flow patterns.

Previous numerical studies of flow in shallow basins have dealt mainly with laboratory configurations [2, 10, 12], and to a lesser extent with real basins [3], using generally 2D depth averaged models. These studies did not examine the effect of different model parameters and options, such as numerical schemes, turbulence models and mesh grid size. The present work focuses on the numerical modelling of flow in shallow rectangular reservoirs with varying boundary conditions [4]. A detailed study of the effects of various user-defined parameters is performed with TELEMAC-2D. Additionally, a comparison between TELEMAC-2D and TELEMAC-3D is conducted for a particular reservoir configuration.

II. DESCRIPTION OF LABORATORY EXPERIMENTAL CASES

Laboratory experiments conducted at Ecole Polytechnique Fédérale de Lausanne (EPFL), Switzerland, are simulated [1]. The experimental setup consisted of a rectangular PVC basin, L = 4.5 m long and B = 4 m wide, and two rectangular free surface channels, l = 1 m long and b = 0.25 m wide each (Figure. 1). The reservoir and channels were at the same bottom elevation. In the present work, one symmetric and three asymmetric cases are simulated, referred to as C-C, L-L, L-R and C-R, respectively. The inlet channel was fed with a clear, constant water discharge of Q = 7 L/s, while a flap gate located at the outlet channel end regulated the flow depth in the reservoir at h = 0.2 m. The horizontal velocity field was measured using UVP transducers placed at 8 cm (= 0.4h) from the bottom. The Froude and Reynolds numbers in the inlet channel are $\mathrm{Fr}_{in} = Q/(bgh^{3/2}) = 0.1$ and $\mathrm{Re}_{in} = V_{in}\,4h/\nu = 4Q/(b\nu) = 112,000$, with g as the gravitational acceleration and V_{in} the flow velocity in the inlet channel.

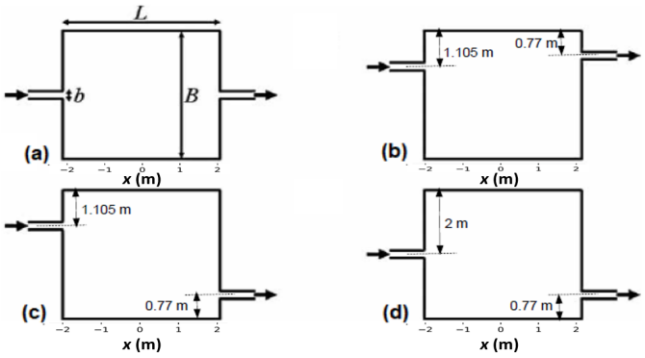

Figure 1. Plane view of laboratory configurations: (a) C-C, (b) L-L, (c) L-R, and (d) C-R. Note the origin of x-axis is taken at middle of the basin.

III. BRIEF DESCRIPTION OF NUMERICAL MODELS

The simulations are performed with the 2D hydrodynamic model TELEMAC-2D [5], which solves the Saint-Venant equations, and the 3D model TELEMAC-3D [5], which solves the Navier-Stokes equations. Several numerical schemes for solving the advection step of velocity and turbulence as well

as several turbulence closure models are available [5]. The Strickler formula is used for the friction term; a value of 80 $m^{1/3}s^{-1}$ (corresponding to PVC) is retained for the bed. The effect of sidewall friction was tested and no influence on the numerical results was noted. For the sake of brevity, results are shown for selected configurations.

IV. 2D-Numerical Study

A. *Effect of numerical schemes*

Using the finite element approach, the method of characteristics, the N scheme, the Positive Streamwise Invariant (PSI) distributive scheme, the PSI scheme with Locally semi-Implicit Predictor-corrector Scheme (LIPS), and the Element by element Residual distributive Iterative Advection scheme (ERIA) for solving the advection step for velocity and turbulence are compared [9, 11]. In all the configurations, a CFL number lower than 0.8 is used; the mesh size is 0.025 m. Figure 2 illustrates measured and computed cross-sectional profiles of the longitudinal velocity for k–ε and Spalart-Allmaras turbulence models for the C-C configuration. The effect of numerical schemes is very weak. This finding remains valid for other reservoir configurations and turbulence models.

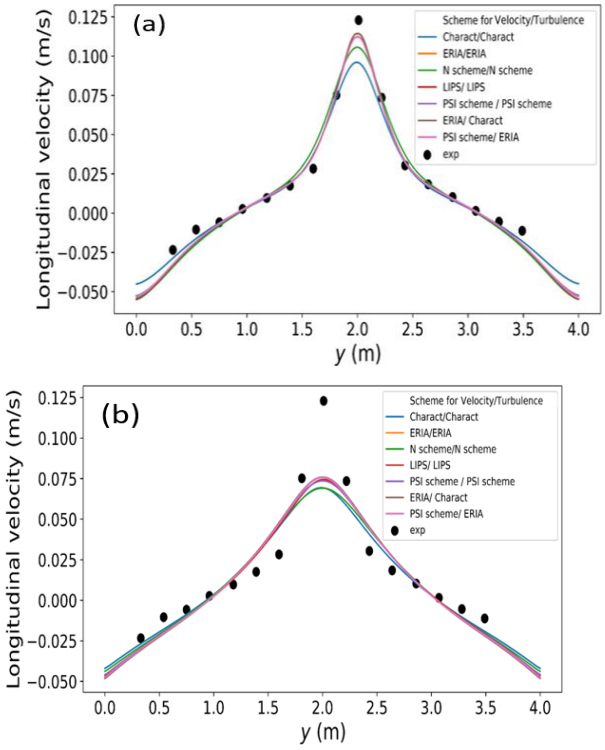

Figure 2. C-C configuration: Results for (a) k–ε turbulence model, and (b) Spalart-Allmaras (SA) turbulence model. Measured and computed cross-sectional profiles of longitudinal velocity at x = 0.71 m using finite element approach, with different numerical schemes for advection. Mesh size of 0.025 m.

Using the finite volume approach, the second order scheme in time and space WAF (Weighted Average Flux) for advection of velocity and turbulence is tested. The CFL number is set at 0.8. The finite volume approach with WAF scheme yields an oscillatory flow pattern that was not observed experimentally (Figure 3). Changing the mesh size (0.0125 m and 0.05 m, instead of 0.025 m) does not improve the numerical results. With this version of TELEMAC-MASCARET (V8P1), the finite element approach provides better results than the finite volume approach.

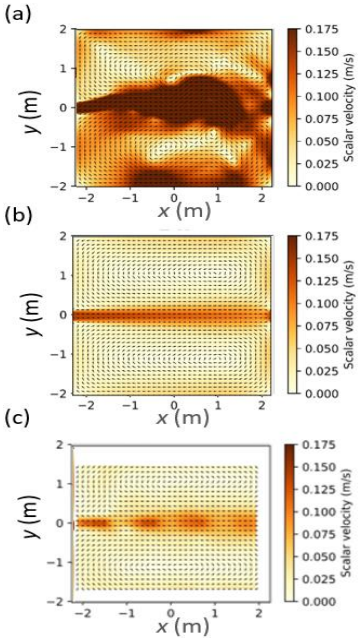

Figure 3. C-C configuration: (a) Oscillatory flow state found using finite volume approach, (b) finite element results, and (c) measurements. Numerical results for k–ε turbulence model, WAF for finite volume and LIPS for finite element for advection of velocity and turbulence. Mesh size of 0.025 m.

B. *Effect of turbulence models*

Using the finite element method, six turbulence models are evaluated: the Spalart-Allmaras (SA) model [6], the standard k–ε model, the constant viscosity model, the Elder model, the Smagorinsky scale model, and the depth-averaged Mixing Length turbulence model. The Locally semi-Implicit Predictor-corrector Scheme (LIPS) is used with a CFL number lower than 0.8 and a mesh size equal to 0.025 m. Model-data comparisons are shown in Figure 4.

The Spalart-Allmaras (SA) model reproduces correctly the measurements for the four configurations (Figure 4b). Spalart-Allmaras, which is one-equation model, has also the advantage to be less computational time consuming, but reproduces less well the velocity magnitude (Figure 2b).

The standard k–ε model reproduces fairly well the velocity magnitude and vector, except for the L-R case, where a flow field with one reattachment point was observed experimentally, but not numerically (Figure 4c). Using a k–ε turbulence model, Camnasio et al. [10] showed that employing a steady flow pattern with lateral reattachment as initial conditions allowed for more satisfactory model-data agreement. Similar results are obtained with TELEMAC-2D (Figure 5).

(a) Experimental

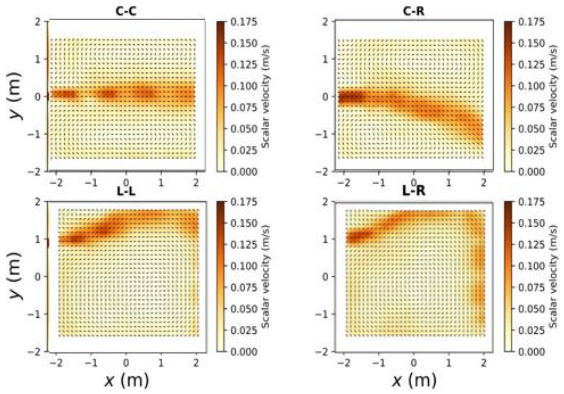

(b) Spalart-Allmaras (SA) turbulence model

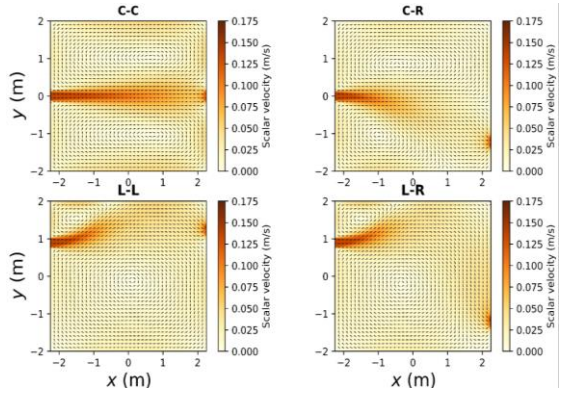

c) k–ε turbulence model

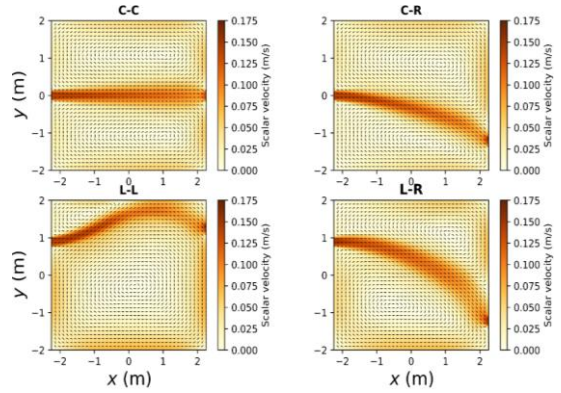

(d) Constant viscosity (10^{-3} m² s^{-1}) turbulence model

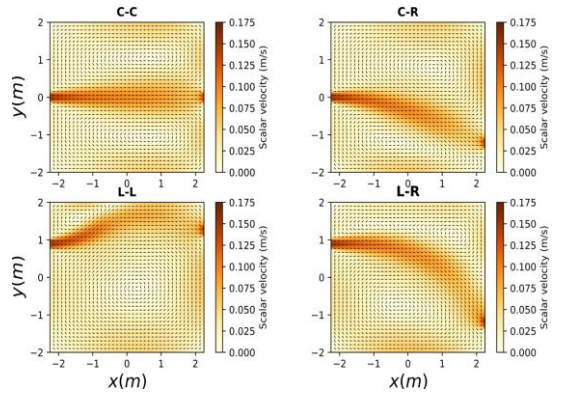

(e) Elder turbulence model

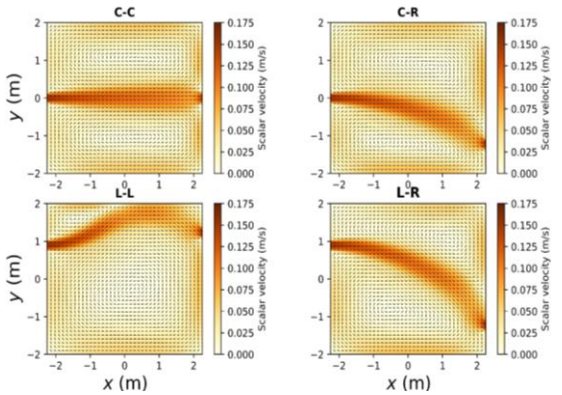

(f) Smagorinsky turbulence model

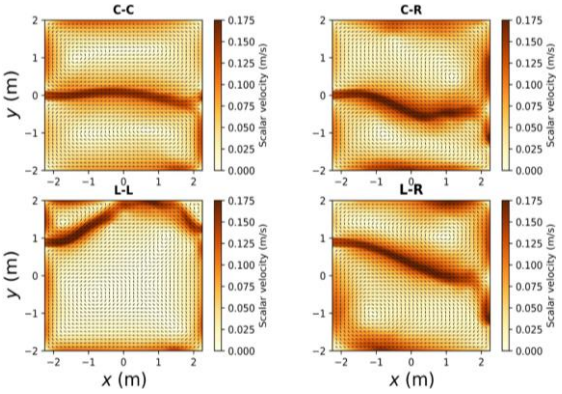

(g) Mixing Length turbulence model

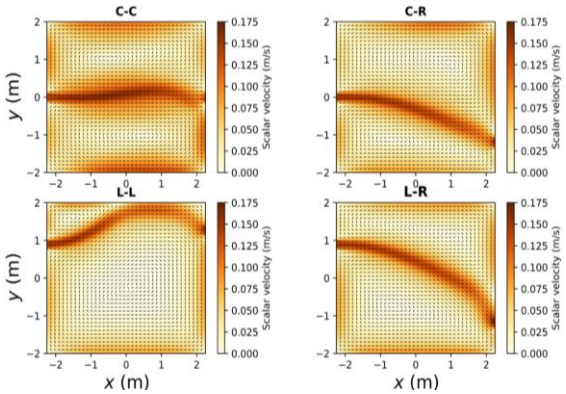

Figure 4. Experimental and computed velocity fields for C-C, C-R, L-L and L-R configurations using different turbulence models (LIPS and mesh size of 0.0025 m).

Various viscosity coefficient values are tested for the constant viscosity (molecular and turbulence viscosity) turbulence model, i.e. 10^{-6}, 10^{-5}, 10^{-4}, 10^{-3}, 10^{-2}, and 10^{-1} m² s^{-1}. Results show that a value of 10^{-3} m² s^{-1} reproduces correctly the velocity magnitude and vectors for C-C, C-R and L-L configurations (Figure 4d), but not for L-R configuration.

The Elder model considers the role of dispersion and includes two coefficients for calculating the longitudinal ($K_l = a_l u_* h$) and transversal ($K_t = a_t u_* h$) diffusion terms (u_* as the shear velocity stress, and a_l and a_t are dimensionless coefficients of

dispersion, set in TELEMAC-2D by default to 6 and 0.6, respectively). Similarly to the standard k–ε and constant viscosity models, Elder's model fails in replicating the flow patterns for the L-R configuration (Figure 4e). The effect of K_l and K_t has been evaluated by changing values of (a_l, a_t): (1, 0.1), (2, 0.2), (3. 0.3), (4, 0.4), (5, 0.5), (7, 0.7), (10, 1). Model-data comparison does not show any noticeable improvement of the results, as illustrated for L-R configuration in Figure 6.

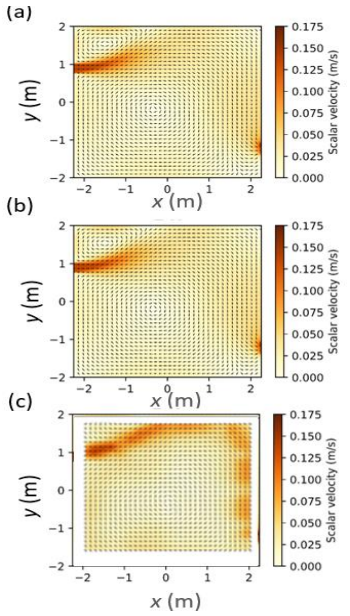

Figure 5. L-R configuration - (a) Initial condition with reattached jet used in TELEMAC-2D simulations, (b) model results obtained at steady state using k–ε turbulence and initial conditions shown in Figure 5a, and (c) measurements. LIPS and mesh size of 0.025 m.

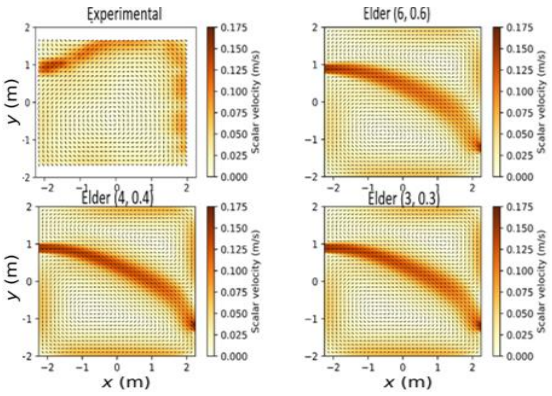

Figure 6. L-R configuration - Computed velocity fields using Elder's turbulence model with different dimensionless coefficients a_l and a_t (LIPS and mesh size of 0.0025 m).

The Smagorinsky scale model calculates the viscosity as $\nu_t = C_s\Delta^2(S_{ij}S_{ij})^{1/2}$, with C_s a dimensionless coefficient to be calibrated, Δ the mesh size derived from the surface, and S_{ij} the stress tensor. This model ignores the effect of dispersion due to heterogeneity of velocities on the vertical direction. The numerical results are not satisfactory (Figure 4f). Using C_s= 0.12, 0.15, 0.18, 0.25, 0.3, or 0.4 instead of the defaults value of 0.2 yields also inaccurate results. The steady state is not reached; an oscillatory state is found which can be due to numerical diffusion (Figure 7).

The Mixing Length turbulence model reproduces correctly the velocity vector maps for C-R and L-L configurations. However, the model does not replicate the steady state for the C-C configuration and the reattachment point observed for the L-R configuration. (Figure 4g).

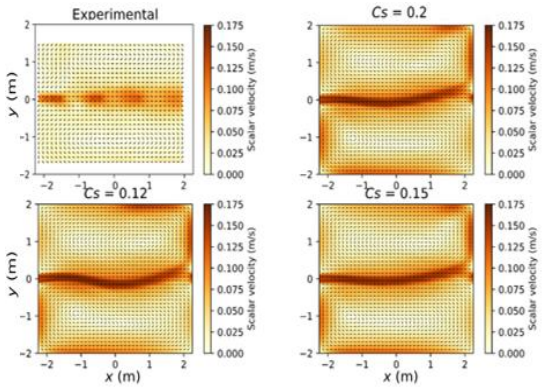

Figure 7. C-C configuration - Oscillatory state found using Smagorinsky turbulence model with C_s=0.12 (LIPS and mesh size of 0.0025 m).

C. *Mesh grid size sensitivity*

A mesh sensitivity is performed with each turbulence model for the C-C configuration. Mesh sizes of 0.0125 m, 0.025 m, 0.05 m, 0.1 m are tested. Results show that mesh size does not improve results for the depth-averaged Mixing Length turbulence model and Smagorinsky model.

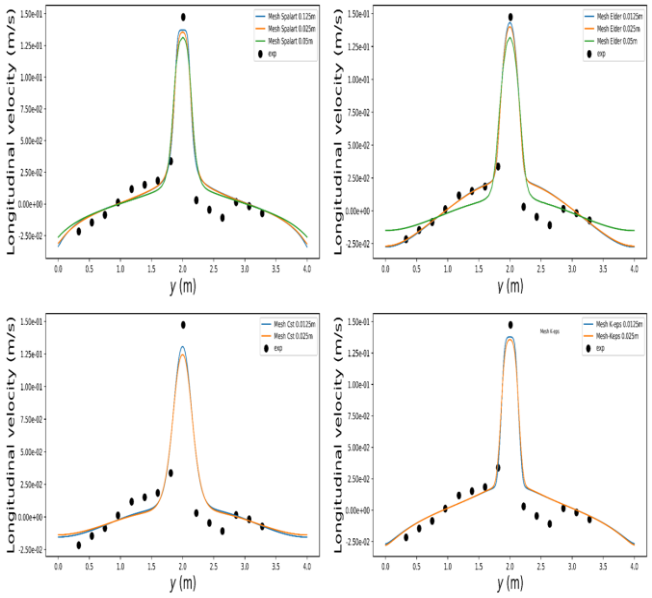

Figure 8. C-C configuration - Measured and computed cross-sectional profiles of the longitudinal velocity at x = 1.73 m using different turbulence models for different mesh sizes. LIPS is used for advection.

Figure 8 shows profiles of the longitudinal velocity at x = 1.73 m for (i) Elder and Spalart-Allmaras turbulence models with mesh sizes of 0.0125 m, 0.025 m and 0.05 m, and for (ii) constant viscosity (10^{-3} m² s^{-1}) and k–ε models with mesh sizes of 0.0125 m and 0.025 m; results with mesh size of 0.05 m are not satisfactory for the flow recirculation features, and thus are not shown for these two models. All the numerical results are obtained using LIPS and a fixed CFL number of 0.8. Overall, the optimal mesh grid size is 0.025 m.

V. TELEMAC - 3D SIMULATIONS

TELEMAC-3D is applied with non-hydrostatic pressure distribution for C-C, L-L, L-R and C-R configurations using k–ε model in both horizontal and vertical directions, and LIPS scheme for advection of velocity and turbulence. The 3D model is composed of five layers uniformly distributed on the vertical, based on 2D unstructured mesh (0.025 m space step). For TELEMAC-3D, the standard k–ε model reproduces correctly the measured velocity vector field for C-C and C-R cases but does not reproduce the reattachment point for L-L and L-R configurations.

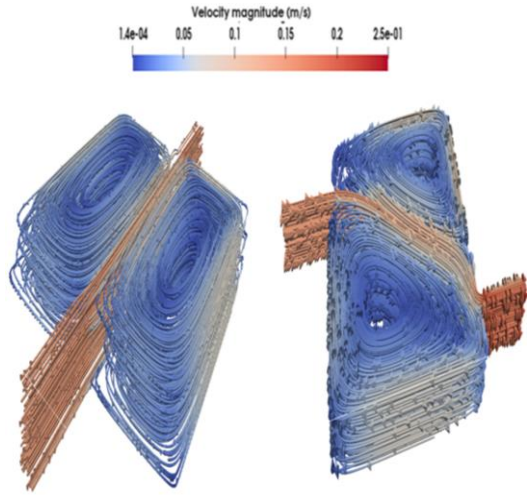

Figure 9. TELEMAC-3D simulations - Streamlines and velocity vectors for configurations C-C (left) and L-R (right) with standard k–ε turbulence model.

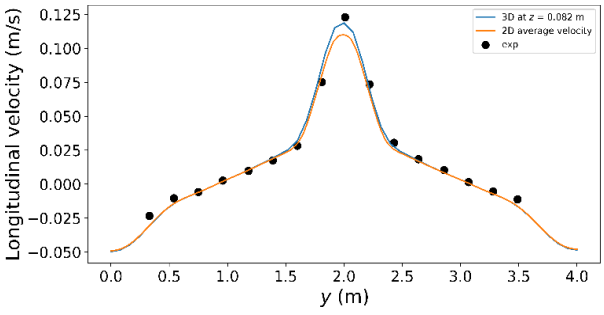

Figure 10. C-C configuration - Measured and computed cross-sectional profiles of longitudinal velocity at x = 0.71 m calculated with TELEMAC-3D and TELEMAC-2D. Results with the standard k–ε turbulence model.

Figure 9 shows the 3D streamlines and velocity vectors for C-C and L-R configurations. Figure 10 compares the experimental velocity recorded at a height of 8 cm from the reservoir bottom with the numerical results of TELEMAC-2D (averaged values) and TELEMAC-3D extracted at a height 8.2 cm. A slightly better results of the peak velocity are obtained by the 3D model.

VI. CONCLUSIONS

A numerical modelling of flow in shallow rectangular reservoirs with varying boundary conditions is performed using TELEMAC-2D and TELEMAC-3D. For TELEMAC-2D simulations, the Spallart-Allmaras turbulence model provides satisfactory results for the four configurations, although it shows a less good representation of the velocity magnitudes in comparison with k–ε, Elder and constant viscosity (10^{-3} m² s^{-1}) models. These three models yield satisfactory results for C-C, L-L and C-R configurations, but do not allow replicating the point of attachment for configuration L-R. The Mixing Length turbulence model reproduces the velocity vectors and magnitude for C-R and L-L configurations only. The effect of numerical schemes for advection of velocity and turbulence is very weak. The mesh sensitivity allows improving the results, but the improvement becomes very weak for mesh sizes less than 0.025 m. TELEMAC-2D and TELEMAC-3D are compared for the particular C-C configuration using the k–ε turbulence model. The 3D simulations slightly improve the results. Future work will complete the current study by quantifying the numerical diffusion, investigating further the effect of initial flow conditions, turbulence in both horizontal and vertical directions and numerical schemes using TELEMAC-3D.

REFERENCES

[1] E. Camnasio, E. Orsi and A.J. Schleiss, “Experimental study of velocity fields in rectangular shallow reservoirs,” Journal of Hydraulic Research, 49(3), 2011, pp. 352-358.

[2] B. Dewals, SA. Kantoush, S. Erpicum, M. Pirotton and A.J. Schleiss, “Experimental and numerical analysis of flow instabilities in rectangular shallow basins,” Environmental Fluid Mechanics, 8, 2008, pp. 31-54.

[3] N. Claude, M. Secher, J. Deng, E. Valette and M. Duclercq, “2D and 3D numerical modelling of the flow and sediment transport in shallow reservoirs: application to a real case,” XXVIth Telemac & Mascaret User Club, 2019.

[4] M. Dufresne, B. Dewals, S. Erpicum, P. Archambeau and M. Pirotton, “Experimental investigation of flow pattern and sediment deposition in rectangular shallow reservoirs,” International Journal of Sediment Research, 25, 2010, pp. 258-270.

[5] J.-M. Hervouet, “Hydrodynamics of free-surface flows- Modelling with finite element method: John Wiley & Sons,” 2007, 341p.

[6] A. Bourgoin, K. El kadi Abderrezzak, S. Benhamadouche and R. Ata, “An adoption of the Spalart-Allmaras turbulence model for two- and three-dimensional free surface environmental flows,” Journal of Hydraulic Research, 59(2), 2021, pp. 314-328.

[7] S.A. Kantoush, “Experimental study on the influence of the geometry of shallow reservoirs on flow patterns and sedimentation by suspended sediments,” PhD thesis, EPFL, Lausanne, Switzerland, 2008.

[8] Y. Peltier, S. Erpicum, P. Archambeau, M. Pirotton and B. Dewals, “Experimental investigation of meandering jets in shallow reservoirs,” Environmental Fluid Mechanics, 14(3), 2014, pp. 699-710.

[9] J.-M. Hervouet, “Residual distribution advection schemes in Telemac,” INRIA. Research Report n°9087, 2013.

[10] E. Camnasio, E. Orsi, S. Erpicum, A.J. Schleiss, M. Pirotton and B. Dewals, “Coupling between flow and sediment deposition in rectangular shallow reservoirs,” Journal of Hydraulic Research, 51(5), 2013, pp. 535-547.

[11] J.-M. Hervouet, “Latest news on distributive advection schemes and dry zones: the ERIA schemes,” Proceedings of the XXIIIrd TELEMAC-MASCARET User Conference, 2016, pp. 201-208.

[12] M. Dufresne, B. Dewals, S. Erpicum, P. Archambeau and M. Pirotton, “Numerical investigation of flow patterns in rectangular shallow reservoirs,” Engineering Applications of Computational Fluid Mechanics. 5(2), 2011, pp. 247-258.